# Energy Reconstruction in a Highly Granularity Semi-Digital Hadronic Calorimeter for ILC Experiments

S. Mannai, K. Manai, E. Cortina, and I. Laktineh

***Abstract*—The Semi-Digital Hadronic CALorimeter (SDHCAL) is one of the two hadronic calorimeter options proposed by the International Large Detector (ILD) project for the future International Linear Collider experiments (ILC). It is a sampling calorimeter with 48 Glass Resistive Plate Chambers (GRPCs) finely segmented into cells of $1\,cm^2$ ensuring a high granularity which is required for the application of the Particle Flow Algorithm (PFA) in order to improve the jet energy resolution which is the corner stone of ILC experiments. The performance of the SDHCAL technological prototype was tested successfully in beam tests at CERN several times. The main point to be discussed concerns the energy reconstruction in SDHCAL. Based on Monte Carlo Simulation of the SDHCAL prototype with Geant4, we will show different analytic energy reconstruction methods used to study the single particle energy resolution and the linearity of the detecor response to pions. In particular, we will highlight a new technique based on the Artificial Neural Network giving promising results compared to the classical analytic methods.**

***Index Terms*—Glass RPC, Hadronic Calorimeter, Semi-Digital, Energy Resolution, Simulation, Neural Network,**

## I. Introduction

THE CALICE collaboration [1] has developed several calorimeter prototypes to evaluate the most appropriate one to be used in the future Linear Collider. One of them is the semi-digital hadronic calorimeter (SDHCAL) constructed in IPNL with the collaboration of many laboratories. After a general description of the SDHCAL technological prototype, the different analytic techniques of energy reconstruction are presented in the third section. The Artifical Neural Network technique for energy reconstruction is detailed in the fourth section followed by a comparison of the Monte Carlo simulation results obtained with the different techniques.

Manuscript received May 31, 2015.

S. Mannai is with Institut de Recherche en Mathématique et Physique (IRMP), Université Catholique de Louvain, 2 Chemin du cyclotron, 1348 Louvain-la-Neuve, Belgium (telephone: +32 10 47 3273, e-mail: sameh.mannai@uclouvain.be).

K. Manai, is with Physics Department. College of Science and Arts. University of Bisha, Bisha, Kingdom of Saudi Arabia (e-mail: manai@ipnl.in2p3.fr)

E. Cortina is with Institut de Recherche en Mathématique et Physique (IRMP), Université Catholique de Louvain, 2 Chemin du cyclotron, 1348 Louvain-la-Neuve, Belgium (telephone: +32 10 47 3273, e-mail: eduardo.cortina@uclouvain.be).

I. Laktineh is with Institut de Physique Nucléaire Lyon (IPNL), Université Claude Bernard, 4 Rue Enrico Fermi, 69622 Villeurbanne, France (telephone: +33 4 72 44 84 57, email: laktineh@ipnl.in2p3.fr)

## II. The SDHCAL prototype

### A. General description

The SDHCAL technological prototype of $1 \times 1 \times 1.3\,m^3$ was conceived and built fulfilling almost all the ILC requirements by associating different technological options. It is a sampling calorimeter made with 48 large Glass Resistive Plate Chambers (GRPC) of $1\,m^2$ area associated with power-pulsed embedded readout electronics [2]. Each GRPC is placed inside a stainless steel cassette hosted by a self-supporting mechanical structure made of 1.5 cm thick plates of stainless steel. The cassette walls and the structure plates form the calorimeter's absorber. The cassette is 11 mm thick where 5 mm for the walls and 6 mm is the GRPC thickness. In total 2 cm of stainless steel is separating two consecutive GRPCs.

### B. GRPC Design

The GRPC (Fig. 1) has two glass plates with a thickness of 0.7 mm and 1.1 mm for the anode and cathode respectively, separated by a 1.2 mm thick gap filled with a gas mixture of 93% of tetrafluoroethane (TFE), 5% of $CO_2$ and 2% of $SF_6$. The first gas provides the primary electrons-ions when ionized by the crossing charged particle while the second and the third are UV photons and electrons quencher respectively. Their role is to limit the size of the avalanche that follows the creation of primary electrons. It also reduces the probability of producing additional avalanches away from the charged particle's impact in the GRPC. Readout pads of area 1cm×1cm are isolated from the anode glass by a thin Mylar foil 50 $\mu$m. These copper pads are etched on one side of a PCB; on the other side are located the front-end readout chips, HARDROC ASICs(HAdronic Rpc Detector ReadOut Chip), that was designed for the readout of the RPC detectors foreseen for SDHCAL [3],[4]. The HARDROC readout is a three-threshold (semi-digital) and has been designed to be power-pulsed by switching on/off the power-hungry parts of the ASICs by sending external control signal and therefore takes advantage of ILC duty cycle expected to be 0.95 ms bunch crossing every 200 ms. This will reduce the power consumption per copper pad from 1.425 mW to less than 0.2 mW. Thus, the SDHCAL power consumption is below 10mW per channel and sufficiently low and therfore a cooling system will not be necessary. Finally, a polycarbonate spacer ('PCB support' in Fig. 1) is used to 'fill the gaps' between the readout chips and to improve the overall rigidity of the cassette (detector/electronics 'sandwich') as well as the lateral

978-1-4799-9918-7/15/$31.00 

homogeneity of the active layer. The total theoretical thickness of the assembly is 5.825 mm. Taking into account air gaps and engineering tolerances, the true thickness was measured and found to be in the vicinity of 6.15 mm.

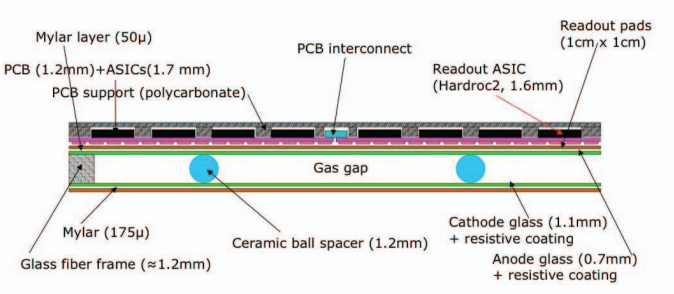


Fig. 1. Schematic cross section view of a GRPC.

### C. SDHCAL performance

SDHCAL has succeed to be a sampling hadronic calorimeter with high granularity in both the transverse and the longitudinal directions with the challenge to cope with the millions of electronic channels needed to read out such a high-granularity and yet still compact and hermetic detector. The technological prototype was tested successfully in beam tests at CERN several times and shows nice performance. Fig. 2 show an event display of the hadronic and electromagnetic showers observed during test beam with SDHCAL. The colors indicate the information related to the three thresholds where red color indicating highest threshold fired pads, blue color indicating the middle threshold and green one that of the lowest one.

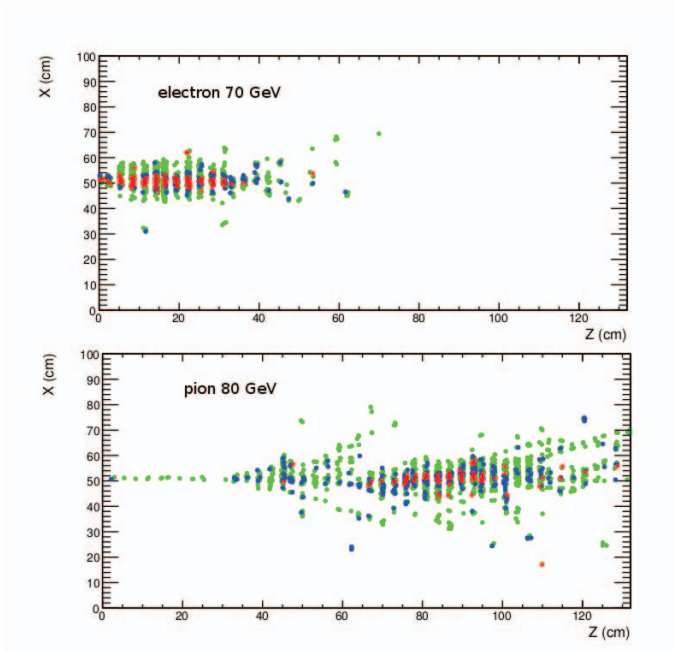


Fig. 2. The shower profile for 70GeV electrons and 80GeV pions. The hits in green color corresponds to the fired pads in the detector when the $1^{rst}$ threshold is crossed, the blue ones when the $2^{nd}$ threshold is crossed and the red ones when the $3^{rd}$ threshold is crossed.

The SDHCAL performance can be characterised by the measurement of the detection efficiency and pad multiplicity. The efficiency of given layer of the detector is defined as the probability to find at least 1 hit withing 3 cm of the muon reconstructed track. The multiplicity is defined as the mean number of hits matched on studied layer within 3 cm of the track impact. Fig. 3 and Fig. 4 shows the measurements of the detection efficiency and pad multiplicity with data taken during test beam at Cern. An efficiency of $\sim 96\%$ is observed over most of the chambers with an average multiplicity of about 1.7.

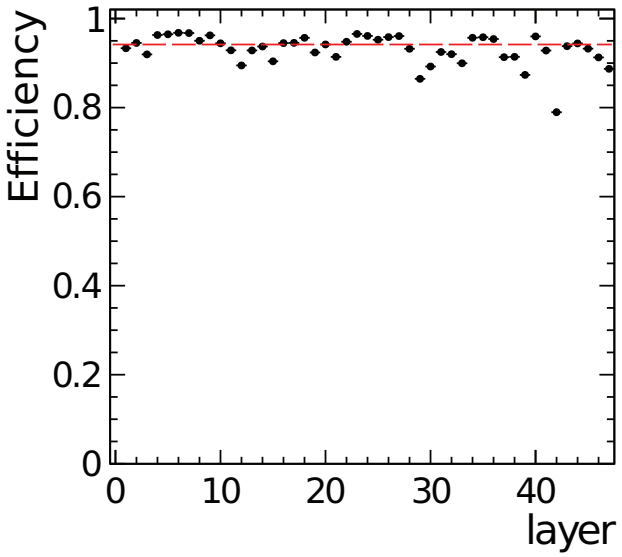


Fig. 3. Detector efficiency.

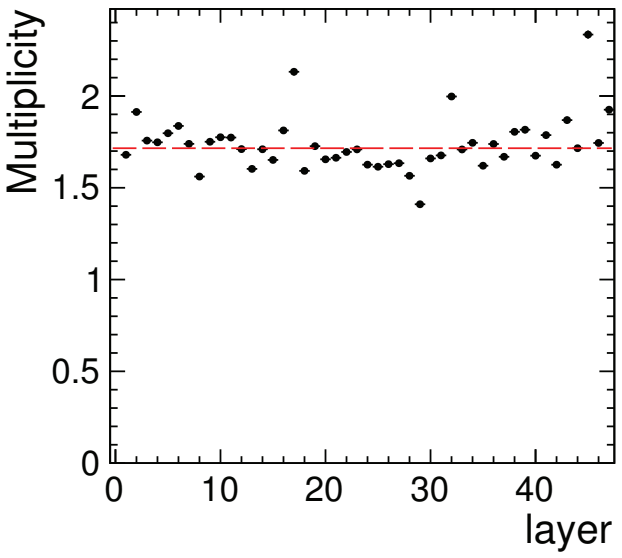


Fig. 4. Pad multiplicity.

## III. Analytic Energy Reconstruction methods

The data samples used in this section have been generated using version 4.9.3 of GEANT4 [5],[6]. We simulated 1000 events of negative pions per energy, betwen 1 and 100 GeV by a step of 1 GeV considering QGSPBERTINI physics list[7],[8].

The pion energy measured in the digital calorimeter is proportional to the number of the fired pads, called "hits", and counted only when the energy is above a given threshold. This concept lead to a deterioration of the response of the calorimeter observed at high energies where the shower core is very dense and we can have up to more than 100 avalanches per $cm^2$ inside the GRPC, when the typical avalance size is $\approx 1mm^2$. Thus a binary readout will suffer from saturation effect. Therefore, we provided a semi-digital approach for the energy reconstruction while using three thresholds instead of one to reduce this effect and improve the energy resolution (Fig. 5). The choice of this semi-digital option rather than the binary one was motivated by simulation studies[9], [10]. To measure the deposited energy in the calorimeter with the semi-digital approach, we count the number of hits over each of the thresholds affected by three weights ($\alpha$, $\beta$, $\gamma$) to obtain the reconstructed energy as:

$$E_{rec} = \alpha \cdot N_1 + \beta \cdot N_2 + \gamma \cdot N_3 \quad (1)$$

$N_1$, $N_2$, $N_3$ represent respectively the number of hits beyond threshold 1 ($S_1$) but below threshold 2 ($S_2$), beyond threshold 2 but below threshold 3 ($S_3$) and beyond threshold 3.

Our strategy of optimisation of the energy resolution in the semi-digital method, consits of two steps. The first one, is the determination of the best thresholds values giving good linearity and energy resolution in the digital case. Thus, the thresholds ($S_1$) and ($S_2$) giving a good linearity can be fixed to 5 and 10 Mips [9]. The third threshold ($S_3$) must be lower, then we use the one giving the best energy resolution which is 0.25 Mip. Once the thresholds are choosen, the second step consists in the determination of the best set of the calibration constants ($\alpha$, $\beta$, $\gamma$) which give us a reconstructed energy closest to the beam energy and allowing a better energy resolution.

To realise the second task we used a minimisation procedure and our minimisation function is a $\chi^2$-like minimisation defined by R:

$$R = \sqrt{\frac{1}{N} \cdot \sum_{i=1}^{N} \frac{(E_{\text{beam}} - (\alpha \cdot N_1 + \beta \cdot N_2 + \gamma \cdot N_3))^2}{E_{\text{beam}}}} \quad (2)$$

Where 'i' is the event number.

To check the validity of the thresholds mentionned above, we tried in the past several values of thresholds to minimise equation 2. $S_1$, $S_2$ and $S_3$ are choosen to varry respectively from 0.1 to 3 Mips, 4 to 8 Mips and 9 to 15 Mips. The minimisation is studied for each energy and the results obtained are of the same order of the values of the thresholds used above.

To perform this analysis a macro written in C++ and based on the root class "TMinuit" [11], has been used and allowed the determination of the calibration constants by the minimisation of equation 2. Once the calibration constants $\alpha$, $\beta$ and $\gamma$ are determined, they are used to calculate the reconstructed energy according to equation 1.

Each reconstructed energy distribution is fitted with a gaussian. Then from the fit parameters we can deduce the standard deviation $\sigma$ and the average reconstructed energy to calculate the energy resolution and the linearity.

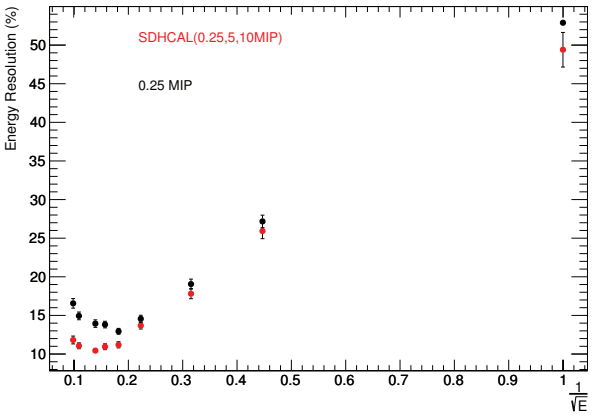


Fig. 5. SDHCAL and DHCAL energy resolution comparison

We used different methods of energy reconstruction to find the best optimisation of the calibration constants described above. These methods depends of the nature of the calibration constants, each offer a modelisation depending or not of the energy of the beam. The comparison between the results obtained with each method will be summarised in Figs. 13 and 14 at the end of this paper.

The first analytic method used is called "Energy Dependent Calibration Constants". In this method, the calibration parameters are supposed to be contants and are optimised independently for each energy. This method shows good results, especially the best linearity compared to the other reconstruction methods but has a drawback which is the dependence of the calibration constants of the beam energy supposed to be unknown.

This lead us to try a second method called "Free Dependent Energy Calibration Constants". In contrast to the first method, in which the minimisation is done energy by energy, this second method consists in minimising equation 2 for all the energies at the same time and thus provide a set of universal calibration parameters.

Nevertheless, inspecting the behaviour of the calibration constants with the first method, we observed that they depend strongly of the energy of the beam and the total number of hits in the detector $N_{\text{tot}}$. Thus it is not allowed to have constant values of $\alpha$, $\beta$ and $\gamma$ for a large energy range. Therefore, we tried a third method of reconstruction called "Quadratic Parametrisation" consiting in the correction of the reconstructed energy formula by replacing ($\alpha$, $\beta$, $\gamma$) with new quadratic parameters with respect to $N_{\text{tot}}$. The new reconstructed energy formula is defined by:

$$E_{rec} = \alpha(N_{tot}).N_1 + \beta(N_{tot}).N_2 + \gamma(N_{tot}).N_3$$

Where:
$\alpha(N_{tot}) = \alpha_1 + \alpha_2.N_{tot} + \alpha_3.N_{tot}^2$
$\beta(N_{tot}) = \beta_1 + \beta_2.N_{tot} + \beta_3.N_{tot}^2$
$\gamma(N_{tot}) = \gamma_1 + \gamma_2.N_{tot} + \gamma_3.N_{tot}^2$

In Fig. 6, the parametrizations of $\alpha$, $\beta$ and $\gamma$ as a function of $N_{tot}$ are presented.

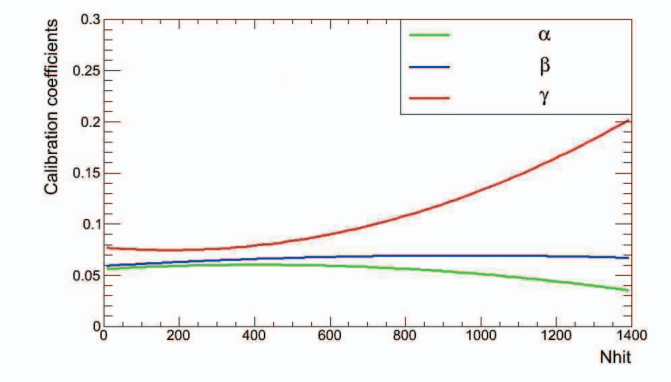


Fig. 6. Evolution of the coefficients $\alpha$, $\beta$ and $\gamma$ in terms of the total number of hits

This last method is adopted as the official method used in the energy reconstruction by SDHCAL. It was used in the publication of the last results of SDHCAL [12].
Furthermore, we used an other technique based on the artificial neural network in order to improve the energy resolution in the hadronic calorimeter.

## IV. Neural Network Energy Reconstruction

### A. General description of the Artificial Neural Network

Artificial Neural Networks (ANNs) are non-linear computational algorithms inspired from biological neural systems of the human brain and based on the same principles [13]. It has been applied in the last years to a wide range of high energy physics experiments and several physics results have been achieved using this method [14–18]. ANNs are well known as a powerful and a reliable analysis tool in the high energy physics community [19–21].

The ANN can be moddeled by a set of input nodes constituting the input layer and receiving the input signals $(x_1, x_2, ..., x_n)$ where each input is normalized and weighted by $w_j (j = 1, ..., n)$, a number of hidden layers and an output layer of computation nodes. The nodes in each layer are connected to the nodes of the neighbouring layers. Each node present a non-linear information processing unit called neuron (Fig. 7). Each input signal $x_j$ connected to neuron k, is multiplied by a synaptic weight $w_{kj}$. A linear combination consists in summing the weighted input signals. Then the activation function is applied to limit the amplitude of the output of the neuron which is usually a sigmoid function. In mathematical terms, the artificial neuron calculation is described by the following equations:

$$u_k = \sum_{j=1}^{n} w_{kj}.x_j \tag{3}$$

$$y_k = \varphi(u_k + b_k) = \varphi(v_k) \tag{4}$$

where $w_{kj}$ are the connections weights and $b_k$ is a bias.

$$\varphi(v) = \frac{1}{1 + exp(-(u_k + b_k))} \tag{5}$$

To obtain the desired output from the network, we should adjust the weights initially random. The algorithm of adjustment is referred to as Learning or Training taking into account the comparison between the output of the network and the desired target corresponding to the training sample. One of the methods widely used for its good performance is called "learning by epoch". It's consisting first in the summation of information for the whole pattern and then updates the weights. Each update minimize the summed error defined by:

$$Error = \frac{1}{2}.\sum_j (d_j - o_j)^2 \tag{6}$$

Where $d_j$ is the desired target and $o_j$ is the output computed by the network. The performance of ANN is given by the accuracy of prediction measured by equation 6 and the convergence of the learning prosess. At the output of the ANN, we have a plot with two error curves. The first represents the error calculated for the training sample called training error and the second curve corresponds to the error calculated to another independent test sample not used in the training then called the generalisation error. The purpose from the learning process is to obtain a low generalisation error caracterising the performance of the ANN to model new data not used in the training.

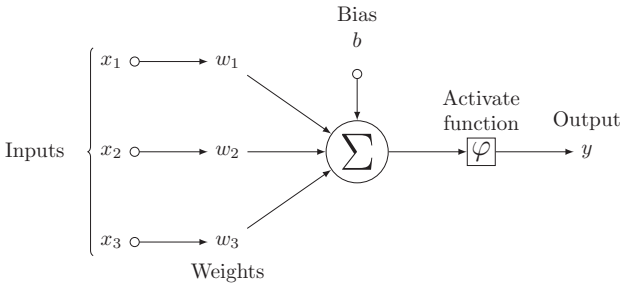


Fig. 7. Example of modelisation of an artificial nurone using three inputs

### B. Energy reconstruction using Neural Network in Monte Carlo simulation

In this study we used the root class TMultiLayerPerceptron to build our neural network [22]. We used here the pions datasets generated with Monte Carlo simulation and used in the previous section to compare the results obtained with the different techniques.
First we identified the optimal ANN architecture by trying

different numbers of neurones in the hidden layers and based on the statistic measurment of the root mean square error defined by:

$$\sqrt{\frac{\sum_i^n (E_\mathrm{i} - P_\mathrm{i})^2}{n}} \tag{7}$$

Where $E_\mathrm{i}$ is the beam energy and $P_\mathrm{i}$ it's predicted value by the neural network. The neural network architecture used in this analysis is illustrated in Fig. 8.

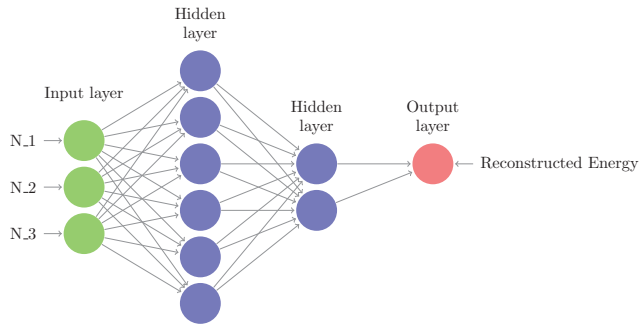


Fig. 8. ANN Architecture used in the analysis.

We found that the most appropriate ANN architecture to the simulation datasets corresponds to two hidden layers with respectively 6 and 2 nodes. The input variables are choosen to be the number of hits related to the 3 thresholds discussed previously: $N_1$, $N_2$ and $N_3$. The behaviour of the input variables with respect to the beam energy is shown in Fig. 9.

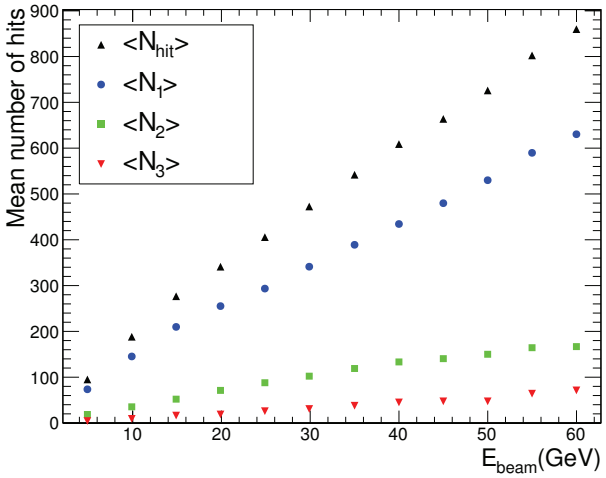


Fig. 9. Average number of hits in the hadronic shower sample corresponding to the first threshold only (blue), to the second threshold but not the third one (green), to the third threshold (red), and to the total number (black) as as a function of the beam energy.

The correlations between the input variables and the real particle energy are automatically learnt during the training of the neural network. The training process was conducted using 50 samples corresponding to the simulated odd energies from 1 to 99 GeV. We used 40 samples during the test process corresponding to the even energies from 10 to 90 GeV.
As a result, from the test samples, the Neural Network should estimate the energy of the incident particle defined as the output variable $E_\mathrm{rec}$. The estimated energies obtained with the ANN technique are presented in Fig. 10.

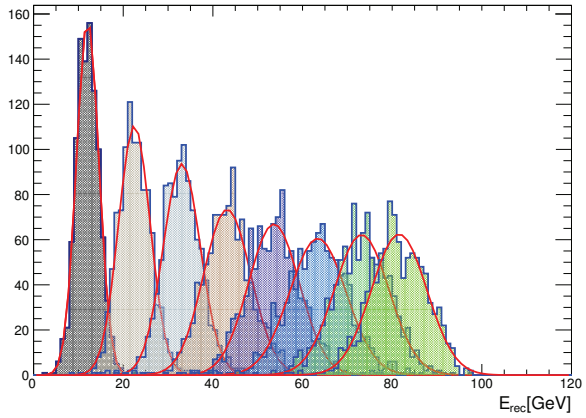


Fig. 10. Pion Energy reconstruction with Neural Network for 10,20,30,40,50,60,70 and 80 GeV.

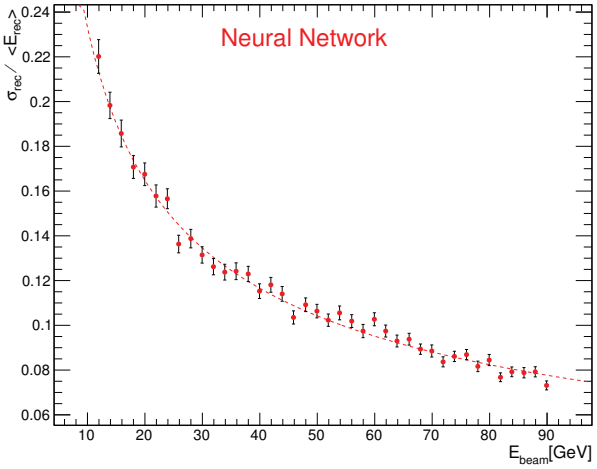


Fig. 11. Pion Energy resolution measured with ANN.

The neural network technique gives a good prediction of the incident energy resulting in a good energy resolution (Fig. 11) and a linearity in the range of $+/-5\%$ (Fig. 12).

The results of this method are promising and achieve an improvement compared to the results obtained from the analytic methods of the energy reconstruction discussed in the previous section. Moreover, with the neural network method of reconstruction we don't use the calibration constants and thus we avoid the difficulties of their parametrisation since, as discussed previously, it's complicated to know the real modelisation of this constants with respect to the energy. Figs. 13 and 14 show a comparison between the results obtained with the different energy reconstruction methods highlighting the goodness of the results obtained with the neural network technique.

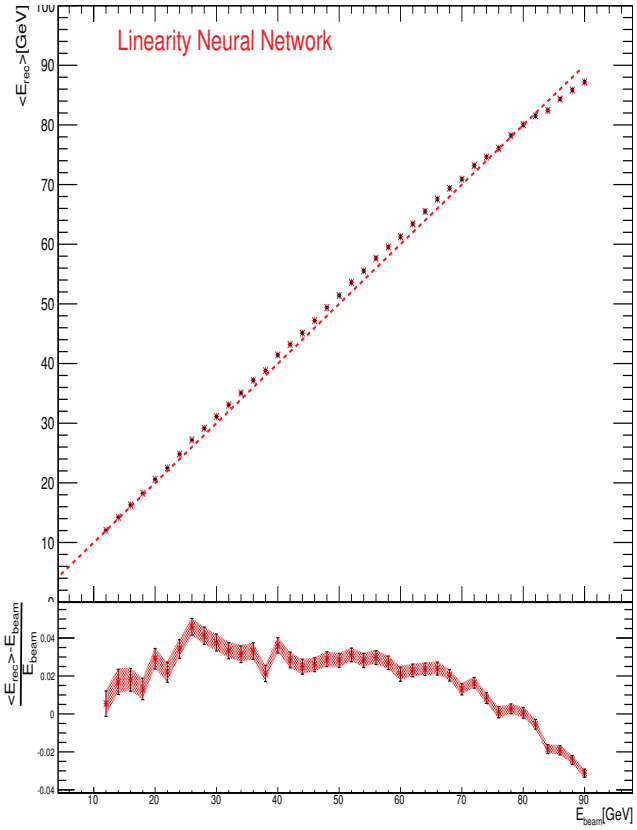


Fig. 12. Pion Mean reconstructed energy measured with ANN. The bottom plot shows the residual non-linearity.

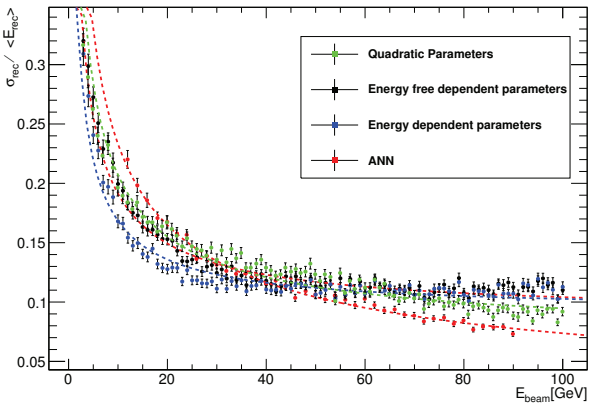


Fig. 13. Comparison of the energy resolution between the different methods of energy reconstruction described in the text.

Preliminary results on energy resolution study with ANN applied to test beam data confirm the promising results observed with the simulation data. With the ANN applied to data samples from 20 to 45 GeV by 5 GeV step taken during December 2014 at Cern, we noticed an improvement on the linearity and the energy resolution reaching 16% at 40 GeV compared to the result obtained with the Quadratic method applied to data taken during 2012 test beam at Cern during 2012 [12]. This result should be confirmed with a study

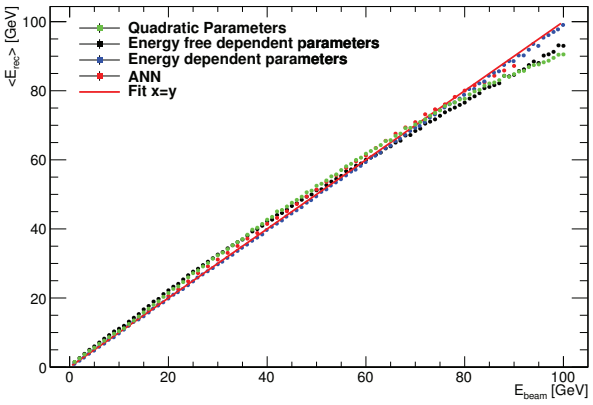


Fig. 14. Comparison of the linearity between the different methods of energy reconstruction. The fit line corresponds to x=y.

covering the whole energy range from 1 to 100 GeV with the data taken during the next test beam at Cern.

## V. Conclusion

The semi-digital hadronic calorimeter prototype has been conceived and built for the future Linear collider experiments. It was tested successfully in tests beam at Cern and a good data quality and stability were observed. Different methods are used in energy reconstruction in SDHCAL in the purpose to improve the detector response to pions. An improvement of the energy resolution could be achieved with the ANN technique with an improved linearity as well. This method has also the advantage of removing the calibration constants parametrisation complexity. The results obtained with the neural network method could be improved by adding input variables related to the hadronic shower topology.

## References


[1] CALICE: http://twiki.cern.ch/CALICE

[2] M. Bedjidian et al, "Performance of Glass Resistive Plate Chambers for a high-granularity semi-digital calorimeter," *J. Instr.*, vol. 6, P02001, 2011.

[3] S. Callier et al., "HARDROC1, readout chip of the Digital HAdronic CALorimeter of ILC," *Nuclear Science Symposium Conference Record, 2007. NSS '07. IEEE 3*, pp.1851-1856, 2007.

[4] S. Callier et al., "ROC chips for imaging calorimetry at the International Linear Collider," *J. Instr.*, vol. 9, C02022, 2014.

[5] J. Allison et al., "Geant4 developments and applications," *IEEE Trans. Nucl. Sci.*, vol. 53, pp.270-278, 2006.

[6] S. Agostinelli et al., "Geant4-a simulation toolkit," *Nucl. Instr. Meth. Phys. Res. A.*, vol. 506, pp.250-303, 2003

[7] Geant4 working group, http://www.geant4.org/geant4/support/proc_mod_catalog/physics_lists/referencePL.shtml

[8] J. Apostolakis et al., "Geant4 Physics Lists for HEP," *Nuclear Science Symposium Conference Record, NSS '08. IEEE*, 2008

[9] S. Mannai, *Energy Reconstruction in GRPC Semi-Digital HCAL*, talk given at CALICE collaboration meeting, September 16-18 2009, Lyon, France http://ilcagenda.linearcollider.org/getFile.py/access?contribId=16&sessionId=1&resId=1&materialId=slides&confId=3642

[10] S. Mannai et al., "High granularity Semi-Digital Hadronic Calorimeter using GRPCs," *Nucl. Instr. Meth. Phys. Res. A.*, vol. 718, pp.91–94, 2013.

[11] TMinuit class, http://root.cern.ch/root/html/TMinuit.html.

[12] CALICE Collaboration, "First results of the CALICE SDHCAL technological prototype," CALICE Analysis Note CAN-037

[13] S. Haykin, "Neural Networks—A Comprehensive Foundation," Prentice-Hall International Inc., New Jerzey, 1999.

[14] R. Fruhwirth, "Computer Physics Communications," , vol.78, pp.23, 1993.
[15] DIRAC experiment, http://www.cern.ch/DIRAC/.
[16] H1 experiment, http://www-h1.desy.de.
[17] P. Abreu et al., *Phys. Lett. B.*, vol. 295, pp.382, 1992.
[18] S. Abachi et al., "Direct measurement of the top quark mass," *Phys. Rev.*, vol. 79, pp.1197, 1997.
[19] BaBar experiment, http://www.slac.stanford.edu/BFROOT/.
[20] CDF experiment, http://www-cdf.fnal.gov/.
[21] DZero experiment, http://www-d0.fnal.gov/.
[22] TMultiLayerPerceptron: Designing and using Multi-Layer Perceptrons with ROOT, http://cp3.irmp.ucl.ac.be/~delaere/MLP/